

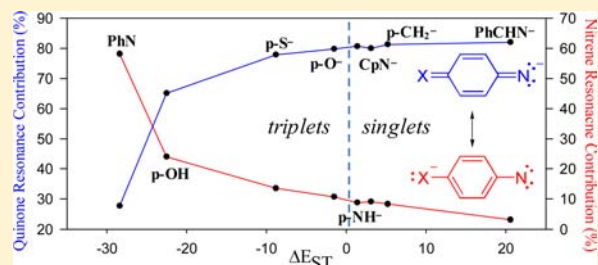
# Anionic Substituent Control of the Electronic Structure of Aromatic Nitrenes

Nathan J. Rau, Emily A. Welles, and Paul G. Wenthold\*

The Department of Chemistry, Purdue University, West Lafayette, Indiana 47907-2084, United States

**S** Supporting Information

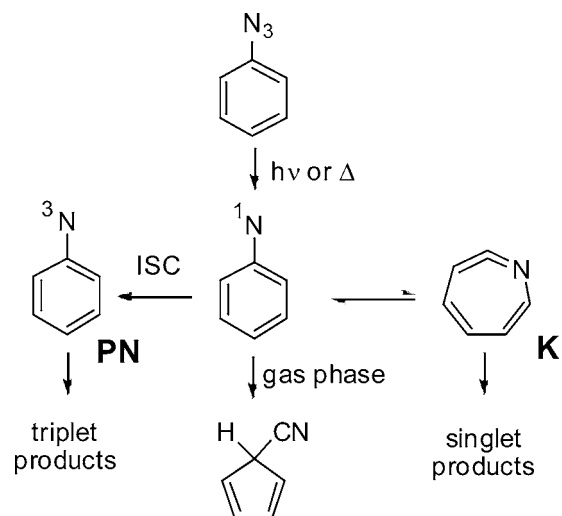
**ABSTRACT:** The electronic structures of phenylnitrenes with anionic  $\pi$ -donating substituents are investigated by using mass spectrometry and electronic structure calculations. Reactions of *para*-CH<sub>2</sub><sup>-</sup>-substituted phenylnitrene, formed by dissociative deprotonation of *p*-azidotoluene, with CS<sub>2</sub> and NO indicate that it has a closed-shell singlet ground state, whereas reactions of *p*-oxidophenylnitrene formed by dissociative deprotonation of *p*-azidophenol indicate either a triplet ground state or a singlet with a small singlet–triplet splitting. The ground electronic state assignments based on ion reactivity are consistent with electronic structure calculations. The stability of the closed-shell singlet states in nitrenes is shown by Natural Resonance Theory to be very sensitive to the amount of deprotonated-imine character in the wave function, such that large changes in state energies can be achieved by small modifications of the electronic structure.



Nitrenes are a fascinating class of electron-deficient and highly reactive intermediates, with electronic structures nominally similar to their carbon analogues, carbenes. Of particular interest is phenylnitrene, which has been the subject of extensive experimental<sup>1–8</sup> and computational studies.<sup>1,8–18</sup> However, while carbenes and nitrenes share some similarities, they exhibit very different reactivity.<sup>4,19,20</sup> For example, phenylcarbene in solution readily forms adducts with alkenes and inserts into C–H bonds, whereas phenylnitrene (PN) gives mostly polymeric tar.<sup>21</sup> The difference in reactivity can be attributed to differences in electronic structures, in particular the structures of the lowest-energy singlet state. Both PN and phenylcarbene are known to be ground-state triplets,<sup>1,4,13,22</sup> but whereas the lowest energy singlet state in phenylcarbene is a closed-shell,  $\sigma^2$  state that is about 2–5 kcal/mol<sup>22,23</sup> above the triplet, the singlet in PN is an open-shell,  $\sigma\pi$  state, with a singlet–triplet splitting of 14.9 kcal/mol<sup>13,24–26</sup> and the  $\sigma^2$  state predicted to be approximately 30 kcal/mol higher than the triplet.<sup>13,25</sup>

The electronic structure of the lowest energy singlet state is important because the singlet nitrene generated by nitrogen loss from the corresponding azide subsequently undergoes intersystem crossing (ISC) to the triplet. Rates of ISC by spin–orbit coupling depend on electronic states because effective ISC requires an orbital transition to create the torque needed to change the angular momentum of the electron.<sup>27</sup> Consequently, favorable ISC requires a change in orbital occupancy in addition to change in the electron spin. For PN, ISC from the  $\sigma\pi$  singlet state to the triplet is slow because it does not involve a change in orbital angular momentum to accompany the change in electron spin.<sup>27</sup> Instead of ISC, the open-shell singlet state of PN can also undergo unimolecular rearrangement, as shown in Scheme 1.<sup>1</sup> In solution, the singlet can ring-expand to form the cyclic ketenimine, K, which can react further. In the gas phase, the

Scheme 1



same singlet undergoes ring contraction to a cyano-substituted 5-membered ring.<sup>2,11,28–31</sup> The products formed in the reaction depend on the relative rates of the competing processes. For singlet PN in solution at temperatures >180 K, ring-expansion occurs faster than ISC, which accounts for the formation of polymeric products. Below 180 K, ISC is favored to form the triplet state, which can then undergo bimolecular reactivity. In contrast, singlet phenylcarbene does not undergo unimolecular rearrangement because ISC is faster under all conditions. One

Received: June 29, 2012

Published: December 31, 2012

strategy for harnessing the reactivity of phenylnitrene is to increase the rate of ISC to prevent unimolecular rearrangement. For example, introducing strong  $\pi$ -donating groups, such as  $-\text{OCH}_3$  and  $-\text{N}(\text{CH}_3)_2$ , in the para position of phenylnitrene has been found to increase the rate of ISC by factors of about 150 and 2500, respectively.<sup>2</sup> Nominally, the increase in the rate of ISC can be attributed to stabilization of the closed-shell singlet state of the nitrene by resonance, as shown in Figure 1, as ISC

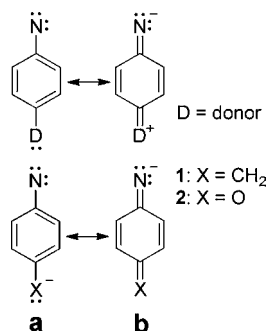
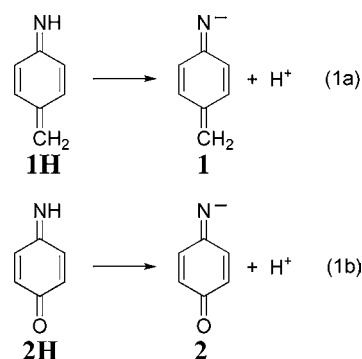


**Figure 1.** Nitrene (a) and quinoidal (b) resonance structures of closed-shell singlet aromatic nitrenes with neutral (D) and anionic (X)  $\pi$ -donating groups.

should be more favorable for the closed-shell singlet state. Computational studies predict that, indeed, addition of a  $\pi$ -donating group at the para position of phenylnitrene stabilizes the closed-shell singlet relative to the triplet, and can increase the rate of ISC.<sup>10</sup> However, the extent of stabilization is not sufficient to overcome the nearly 30 kcal/mol energy gap between the states in the unsubstituted system, nor even the difference between the closed-shell and open-shell singlet states, which is approximately 15 kcal/mol.<sup>10</sup> The reason strong  $\pi$ -donors fail to lower the energy of the closed-shell singlet enough to change the state ordering in aromatic nitrenes is due in part to the diminishing returns that the singlet encounters because of increased zwitterionic character, as shown in the quinoidal structure (structure b) in Figure 1.<sup>2</sup>

In this work, we examine the use of anionic  $\pi$ -donating groups to stabilize the closed-shell singlet state of aromatic nitrenes (Figure 1). Stable, closed-shell singlet states have been found previously in acylnitrenes, where they can even be the ground state of the system.<sup>32</sup> Computational studies of formylnitrene suggest that the stabilization of the closed-shell singlet state results from a weak bonding interaction between the oxygen and nitrogen atoms, indicated by a 0.464 Å shorter N–O distance in the singlet than in the triplet.<sup>33</sup> This stabilization occurs without polarization, and therefore avoids unfavorable charge separation. Similarly, anionic  $\pi$ -donating groups, which do not create charge separation in the quinoidal resonance structures, would also be able to stabilize the closed-shell singlet state of aromatic nitrenes, and even create aromatic nitrenes with closed-shell singlet ground states. By using mass spectrometry, we have carried out an investigation of phenylnitrenes with  $\text{CH}_2^-$  and  $\text{O}^-$  substituents (**1** and **2** in Figure 1, respectively). In one respect, **1** and **2** can be viewed as merely the conjugate-base anions of quinone- and quinomethane imines, **1H** and **2H**, respectively (eq 1b), as reflected by resonance structure (b) in Figure 1. Benzoquinone imines are formed upon the oxidation of aminophenols, either by chemical oxidation<sup>34–39</sup> or under electrochemical conditions,<sup>40–45</sup> and N-substituted benzoquinone imines can be reduced under single-electron transfer conditions,<sup>46,47</sup> but the deprotonation of **1H** or **2H** has not been reported.



Whereas **1** and **2** can be considered the conjugate bases of **1H** and **2H**, respectively, they can also be viewed as substituted aromatic nitrenes, as shown in Figure 1a, and therefore would be expected to have low-lying triplet electronic states. In this work, we show that either state can be obtained, depending on the strength of the  $\pi$ -donating group. Experimental and computational evidence indicates that deprotonated benzoquinomethanimine, **1**, has a singlet ground state in the gas phase, whereas **2**, with a weaker  $\pi$ -donating group, is likely a ground-state triplet, with an electronic structure similar to that of phenylcarbene. The results highlight how substitution and other external factors can be used to tune the electronic structure of aromatic nitrenes.

## EXPERIMENTAL SECTION

All experiments were performed on a flowing-afterglow triple-quadrupole mass spectrometer, which has been described in detail previously.<sup>48</sup> Briefly, hydroxide and fluoride are formed in the source region by 70 eV electron ionization and are carried down a 1 m long flow-tube by helium carrier gas (0.4 Torr, flow  $[\text{He}] = 190 \text{ STP cm}^3/\text{s}$ ). Hydroxide is formed by ionization of a 1/2 mixture of  $\text{N}_2\text{O}$  and methane, and  $\text{F}^-$  is formed by ionization of  $\text{F}_2$  (5% in He). The helium carrier gas is at room temperature and thermalizes the ions in the flow-tube. Ions are allowed to react with neutral reagents that are added through fixed-position inlets downstream in the flow reactor. At the downstream terminus of the flow-tube, ions are sampled through a 1 mm diameter nosecone orifice that is held at 0.2–1.5 V, and focused through a set of four electrostatic lenses. Ions are then analyzed by a triple-quadrupole mass spectrometer and detected using a single channel continuous dynode electron multiplier. The triple quadrupole analyzer used in this work discriminates against low mass ions and is impractical for detecting charged species with  $m/z$  values below 10 Da.

Pseudo first-order reaction rate constants are determined from a plot of the reactant ion depletion versus the flow rate of the neutral reagent, which is added through a ring inlet at a fixed distance (38 cm) from the nosecone. The reported rate constants are the average of replicate measurements and have estimated uncertainties of  $\pm 50\%$ .<sup>48</sup> Reaction rates are also reported in terms of reaction efficiency, which is the ratio of the measured reaction rate,  $k_{\text{obs}}$ , to the collision rate,  $k_{\text{coll}}$ , calculated by using the parametrized trajectory model of Su and Chesnavich.<sup>49</sup> Branching ratios for reactions with multiple observed products were determined by extrapolating the measured branching ratios to zero flow.

Because the flow-tube contains a mixture of ions, reactions were also examined in the second quadrupole of the mass spectrometer to verify the source(s) of the products. In these experiments, a reactant ion is isolated in the first quadrupole, producing an isobarically pure ion beam, which is then allowed to react with a neutral reagent in the second quadrupole, and then the reaction products are monitored with the third quadrupole. For these reactions, the pole offset of the second quadrupole is kept near 0 V, for near thermal reactions. All of the assigned products are observed in the flow reactor and with the mass selected ions.

## MATERIALS

Precursor molecules *m*- and *p*-azidotoluene and *m*- and *p*-azidophenol were synthesized from the corresponding toluidines

and aminophenols, using a procedure based on literature methods.<sup>50,51</sup> All other materials were used as received unless specifically indicated otherwise. Gas purities are as follows: He (99.995%), NO (98.5%), N<sub>2</sub>O (99.0%), CO<sub>2</sub> (99.999%), Ar (99.997%), CS<sub>2</sub> (~99%), and CH<sub>4</sub> (99.0%). The helium carrier gas is further purified by passing the gas through a molecular sieve packed coil immersed in liquid nitrogen. Caution: Azides are potentially explosive and should be handled with appropriate safety precautions. We have not encountered any complications with the aromatic azides used in this work.

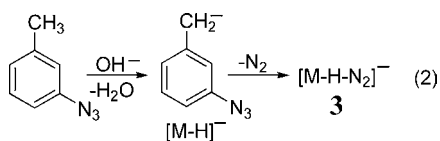
## COMPUTATIONAL DETAILS

Unless otherwise noted, electronic structure calculations were carried out by using the BLYP or B3LYP approaches. Geometries and energies of the triplet and closed-shell singlet states of nitrenes were optimized using a 6-311++G(3df,2p) basis set. In general, the BLYP calculations gave results slightly more favorable to the singlet states than did B3LYP. Getting the self-consistent field for the closed-shell singlet states to converge proved to be challenging with the BLYP calculations, and generally required use of a quadratic conversion approach with an ultrafine grid. Reported energies correspond to 0 K energies, with the zero-point energy corrections calculated by using B3LYP/6-31+G\* geometries and frequencies (unscaled). Potential energy surfaces were calculated at the B3LYP/6-31+G(d) level of theory and are not ZPE corrected. Transition states were verified to be saddle points on the surface by the presence of a single imaginary frequency. Natural resonance theory calculations<sup>52–54</sup> were carried out on the HF/6-311++G(d,p) wave function at the BLYP geometry. Calculations were carried out using Gaussian 03<sup>55</sup> and QChem.<sup>56</sup>

## RESULTS

Reaction of *p*-azidotoluene or *p*-azidophenol with OH<sup>−</sup> results in the formation of three main anionic products. On the basis of their mass-to-charge ratios, two of the products are assigned to be [M–H]<sup>−</sup>, which results from proton transfer, and [M–H–N<sub>2</sub>]<sup>−</sup>, which nominally corresponds to proton transfer accompanied by nitrogen loss to give the *p*-substituted phenylnitrene anions, 1 or 2, respectively. A third major ion has an *m/z* ratio that corresponds to [M+OH–N<sub>2</sub>]<sup>−</sup>, which can be considered as resulting from addition of hydroxide and loss of N<sub>2</sub>; alternatively, it can be considered as a cluster between ion 1 or 2 and water. Ion 2 and its HF cluster can also be formed with F<sup>−</sup> as the base. As is observed in the reactions to form 1 and 2, reaction of *m*-azidotoluene with OH<sup>−</sup> also results in the formation of [M–H]<sup>−</sup> and [M–H–N<sub>2</sub>]<sup>−</sup> (eq 2). Nominally, the [M–H–N<sub>2</sub>]<sup>−</sup> ion, 3, could correspond to the *meta*-isomer of the aromatic nitrene, but the results described below suggest it does not have a nitrene structure. The reaction of *m*-azidophenol by either OH<sup>−</sup> or F<sup>−</sup> results only in the formation of a proton transfer product, [M–H]<sup>−</sup>, but does not occur with additional loss of N<sub>2</sub> under flowing afterglow conditions. Chemical ionization mass spectra for all four reactants are provided as Supporting Information.

Upon ionization of the azides, we also observe the formation of ions that correspond to [M–N<sub>2</sub>]<sup>−</sup>, which are likely the nitrene radical anions formed by dissociative electron capture.



The electronic structures of ions 1, 2, and 3 were examined by using ion/molecule reactions. The measured reaction

efficiencies, observed products, and branching ratios are summarized in Table 1.

**Table 1. Results for Reactivity Studies of Anion-Substituted Aromatic Nitrenes**

reagent	result <sup>a</sup>	ion		
		<i>p</i> -CH <sub>2</sub> <sup>−</sup> (1)	<i>p</i> -O <sup>−</sup> (2)	<i>m</i> -CH <sub>2</sub> <sup>−</sup> (3)
O <sub>2</sub>	efficiency	0.002	0.001	0.088
	[M+O <sub>2</sub> –NO] <sup>−</sup>	<i>b</i>	100%	<i>b</i>
NO	efficiency	0.608	0.505	0.412
	[M+NO] <sup>−</sup>	100%	62%	100%
	[M+NO–N <sub>2</sub> ] <sup>−</sup>	0	38%	0
CS <sub>2</sub>	efficiency	1.204	0.356	0.948
	SCN <sup>−</sup>	(0.243) <sup>c</sup>	(0.157) <sup>c</sup>	(0.664) <sup>c</sup>
	[M+CS <sub>2</sub> ] <sup>−</sup>	96%	88%	0
		4%	12%	100%

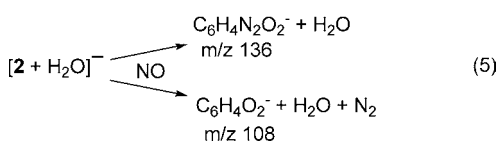
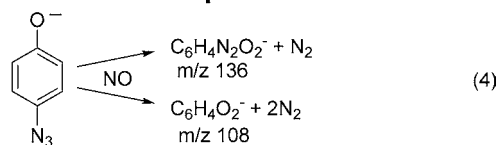
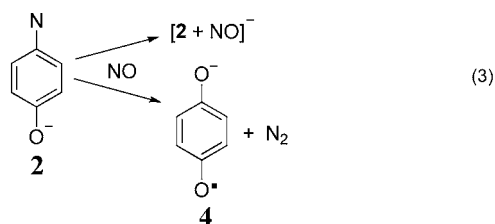
<sup>a</sup>Reaction efficiencies ( $k_{\text{obs}}/k_{\text{coll}}$ ) and observed reaction products; efficiencies based on the rates of reactant ion disappearance, unless noted. <sup>b</sup>No ionic products are observed for these reactions. <sup>c</sup>Efficiencies based on the rates for observed product formation.

Significant differences are observed in the reactions of ions 1–3 with O<sub>2</sub>, NO, and CS<sub>2</sub>. Ions 1 and 2 both react very slowly with O<sub>2</sub>, but with different outcomes. The only observed product from the reaction of 2 and O<sub>2</sub> results from a net nitrogen–oxygen exchange forming semiquinone radical anion (4), whereas no products can be detected for reaction with 1. Similarly, reaction of O<sub>2</sub> with 3 does not produce any detectable products, although it occurs slightly more rapidly.

Ions 1–3 react efficiently with nitric oxide, although there are again differences in products. Ions 1 and 3 react with NO only by addition, whereas 2 reacts with NO by addition and by nitrogen–oxygen exchange, nominally resulting in the formation of 4 (eq 3). It should be noted that the branching ratio for the products in the reaction of 2 with NO, shown in Table 1, is based on flow-tube results. Upon examining reactions with mass selected ions in the second quadrupole, we have found that both of the observed products can also be formed from other ions in the flow-tube, as shown in eqs 4 and 5. The isobaric products observed in the reaction with deprotonated azidophenol are likely the same as those formed from 2 and therefore may affect the measured branching ratio.

Reactions of ions 1–3 with CS<sub>2</sub> have also been examined. With this reagent, ions 1 and 2 undergo reactivity similar to each other and distinct from that for 3. With 1 and 2, the major product observed is NCS<sup>−</sup> (*m/z* 58), resulting from sulfur–nitrogen exchange, and only a small amount of adduct is formed. However, with ion 3 only CS<sub>2</sub> adduct is observed, with no NCS<sup>−</sup> formation.

A surprising result is observed for the reaction of 1 with CS<sub>2</sub>. As indicated in Table 1, the reaction rate, measured by monitoring the depletion of reactant, is found to be about 20% faster than the collision rate. Moreover, although two products are listed in Table 1, the yields of the observed products account for only 20% or so of the reactant ion loss. While exact accounting between reactant and product is not expected due to differences in flow dynamics for different mass ions, the discrepancy is much larger than is typical. We attribute the discrepancy between ion loss and ion formation to a reaction channel that does not produce detectable ions. Most commonly, this would be a reaction that ultimately



results in electron detachment, but it can also occur when the product is formed in an excited electronic state that is unstable with respect to electron loss as in the reaction between phenyl anion and NO.<sup>57</sup>

As noted in the Experimental Section, the estimated uncertainties for rate constants measured in the flowing afterglow are  $\pm 50\%$ . Therefore, the fact that the measured reaction efficiency is greater than 1.000 may be simply due to systematic error in the kinetics measurements. However, reactions that occur faster than the calculated collision rate are known to occur.<sup>58</sup> Typically, these reactions involve electron transfer, which can occur at a larger collision radius than in normal bimolecular reactions. Consequently, an alternate explanation for the greater than unity efficiency of the reaction of **1** with CS<sub>2</sub> is that there is an undetected reaction channel that occurs by electron transfer in addition to observed processes. The reaction cannot be just electron transfer, however, because we do not observe CS<sub>2</sub><sup>-</sup> as a product. Therefore, the reaction likely would proceed by subsequent reaction of CS<sub>2</sub><sup>-</sup> with the radical product of electron transfer within the collision complex.

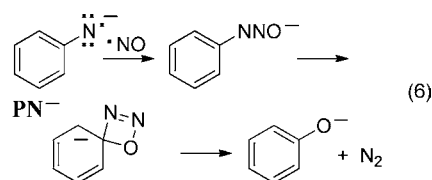
Despite being highly speculative, the electron transfer-initiated reaction mechanism described above also accounts for the outcome in the reaction of **2** with CS<sub>2</sub>. As with the reaction of **1**, the yield of observed ionic products is much less than expected given the extent of reactant ion loss, suggesting the presence of an undetected reaction process. By measuring the kinetics for product formation, the undetected reaction accounts for approximately 55% of the total rate of the reaction. In contrast, unlike what was found for the reaction of **1**, the reaction does not occur faster than the collision rate. However, because the electron binding energy in **2** is expected to be larger than that in **1**, a slower rate of electron transfer would be expected with **2** as compared to **1**.

As shown in Table 1, the rate obtained by monitoring the products in the reaction of CS<sub>2</sub> with **3** is more comparable to that obtained by monitoring loss of reactant, and there is not a significant difference considering the estimated uncertainties. Therefore, although it is possible there is an undetected reaction pathway in the reaction between **3** and CS<sub>2</sub>, it is not as evident as it is in the reaction of **1**, and to a lesser extent, **2**. Regardless, because there are no observable products, and given the range of possibilities for the mechanism, we are unable to suggest any possible structures for any of the undetected channels. Fortunately, the structure assignments discussed in

the following section do not rely on knowing the structures of the products, nor even whether the reactions occur at all.

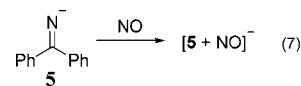
## DISCUSSION

The reactivity observed for ions **1**, **2**, and **3** provides insight into their electronic structures. In this section, we consider the electronic structures in light of the ion reactivity, compare the conclusions with theoretical predictions, and describe computational results that provide further insight into the origins of the effects.



The most important results are found for the reactions with NO. Nitric oxide is a versatile reagent for the investigation of electronic structure of negative ions. With closed-shell anions, it can react as an electrophile, and addition is commonly observed.<sup>59,60</sup> However, because it is also a free radical with a very low electron affinity,<sup>61</sup> it is able to undergo radical reactions without competing electron transfer, and often exhibits characteristic reactivity with open-shell anions.<sup>62–67</sup> For example, phenyl nitrene radical anions, including PN<sup>-</sup><sup>68</sup> and even the methylphenyl nitrene [M–N<sub>2</sub>]<sup>-</sup> radical anions formed in this work, react with NO by nitrogen–oxygen exchange to form the corresponding phenoxides. As shown for PN<sup>-</sup> in eq 6, the reaction is proposed to proceed by initial coupling of the NO radical with the in-plane ( $\sigma$ ) radical of the anion, followed by substitution via a 4-centered transition state. The key to the reaction is that the exothermicity of the initial bond formation (approximately 70 kcal/mol) is more than sufficient to overcome the 41 kcal/mol barrier for the 4-centered transition state.<sup>68</sup> Nitrogen–oxygen exchange is not observed for **1**, despite the fact that the computed energetics for the reaction (see the Supporting Information) are similar to those calculated for PN<sup>-</sup> and benzylnitrene radical anion.<sup>68</sup> The formation of adduct as the only product in the reaction of **1** with NO is consistent with what is expected for a closed-shell anion, and is expected for an ion with a quinoidal structure, such as that shown in **1b**. For comparison, the reaction of deprotonated benzophenone imine (**5**) with NO also gives adduct as the only ionic product (eq 7), consistent with its closed-shell electronic structure.

In contrast, reaction of **2** with NO gives a nearly 60/40 mixture of adduct and the semiquinone anion (eq 3), which results from nitrogen–oxygen exchange. We interpret the nitrogen–oxygen



exchange reaction to indicate an open-shell electronic structure similar to that of PN<sup>-</sup>, with an in-plane,  $\sigma$  radical localized on the nitrogen. The open-shell electronic state can either be triplet or singlet, but preliminary spin-flip calculations (see the Supporting Information) find the triplet state lower in energy, 12.8 kcal/mol below the open-shell singlet. Therefore, on the basis of the ion reactivity with NO, we propose that **1** is a ground-state closed-shell singlet, and that **2** is a ground-state triplet.<sup>69</sup> Moreover, although

the reaction is very slow, nitrogen–oxygen exchange is also the only product observed in the reaction of **2** with molecular oxygen, consistent with the triplet assignment.

The state assignments for **1** and **2** deduced from the reactions with NO are consistent with theoretical calculations. The computational results are summarized in Table 2. At the

**Table 2. Calculated Singlet–Triplet Splittings and Resonance Structure Contributions for *p*-Substituted Phenylnitrenes and Other Nitrene Derivatives**

<i>para</i> -substituent (unless otherwise indicated)	$\Delta E_{ST}^a$	%nitrene <sup>b</sup> (structure a)	%quinoidal <sup>b</sup> (structure b)
–H (PN)	–29.1	58.1	27.7
–OH	–22.5	24.0	65.1
–CO <sub>2</sub> <sup>–</sup>	–23.5 <sup>c</sup>	22.5	71.2
–S <sup>–</sup>	–9.0	13.5	77.9
–O <sup>–</sup> ( <b>2</b> )	–2.0	10.7	79.8
	–2.9 <sup>d</sup>		
–NH <sup>–</sup>	0.7	8.8	80.7
–CH <sub>2</sub> <sup>–</sup> ( <b>1</b> )	4.2	8.3	81.3
C <sub>5</sub> H <sub>4</sub> N <sup>–</sup> ( <b>7</b> ) <sup>c</sup>	2.4	9.1	80.0
PhCHN <sup>–</sup>	19.7	3.1	82.0

<sup>a</sup>Adiabatic energy differences between the triplet states and the closed-shell singlets; values in kcal/mol, calculated at the BLYP/6-311++G(3df,2p) level of theory, unless otherwise noted, corrected for ZPE differences; values < 0 indicate ground-state triplets. <sup>b</sup>Calculated for the singlet by using NRT with the HF/6-311+G(d,p) wave function at the BLYP optimized geometry; see the Supporting Information for analysis details. <sup>c</sup>Calculated at the B3LYP/6-31+G(d) level. <sup>d</sup>Calculated at the spin-flip CCSD(T)/cc-pVDZ level; see the Supporting Information. The open-shell singlet at this level of theory is 12.8 kcal/mol higher than that of the triplet. <sup>e</sup>Cyclopentadienyl nitrene anion.

BLYP/6-311++G(3df,2p) level of theory, the energy difference between the closed-shell singlet and triplet states of **1** is calculated to be about 4 kcal/mol, with the singlet being the ground state. However, ion **2** is predicted to have a triplet ground state, with a singlet–triplet splitting of 2.0 kcal/mol.

Therefore, the calculations predict that **2** has an electronic structure similar to that of phenylcarbene, suggesting that nitrenes generated from azidophenoxide salts should react more like carbenes than noncharged aromatic nitrenes. Condensed-phase studies of the azidophenoxide salts are in progress.

The difference in the relative stabilities of the singlet states of **1** and **2** can readily be attributed to differences in the  $\pi$ -donating strengths of the CH<sub>2</sub><sup>–</sup> and O<sup>–</sup> moieties, as the stronger  $\pi$ -donating group better stabilizes the singlet. This trend is reflected in the left column of Table 2, which shows the computed energy differences between the triplet and closed-shell singlet states for a series of aromatic nitrenes. Stronger  $\pi$ -donors better stabilize the closed-shell singlet state as expected, even among the anionic groups. The closed-shell singlet stability ordering follows the trend CH<sub>2</sub><sup>–</sup> > NH<sup>–</sup> > O<sup>–</sup> > S<sup>–</sup>, which mirrors the stability of the aromatic anions, as reflected by the relative acidities of toluene, aniline, phenol, and thiophenol. In contrast to the results for **1** and **2**, the calculations predict that a carboxylate group does not have a large effect on the singlet–triplet splitting of aromatic nitrenes. However, this is not unexpected considering the present work, because the carboxylate group is not a strong  $\pi$ -donating substituent.

The reactions of **1**, **2**, and **3** with CS<sub>2</sub> have also been examined, but provide less insight into the electronic structures. For all of the ions, reactions result in formation of adducts, but

with **1** and **2** the major product is NCS<sup>–</sup>, resulting from sulfur–nitrogen exchange. Formation of NCS<sup>–</sup> has been observed previously in the reaction of CS<sub>2</sub> with N<sub>3</sub><sup>–</sup>,<sup>70</sup> and we have found that it is also formed as a minor product (20%) in the reaction of CS<sub>2</sub> with **5**.

The mechanism of NCS<sup>–</sup> formation in the reaction with **1** or **2** likely involves simple addition of CS<sub>2</sub> to form an adduct, followed by substitution via a 4-centered transition state. This mechanism is similar to that proposed previously for the reaction of CS<sub>2</sub> with N<sub>3</sub><sup>–</sup>.<sup>70</sup> The computed potential energy surface for the sulfur–nitrogen exchange with **1** and **2** is shown in Figure 2. Energies for the intermediate state and rearrange-

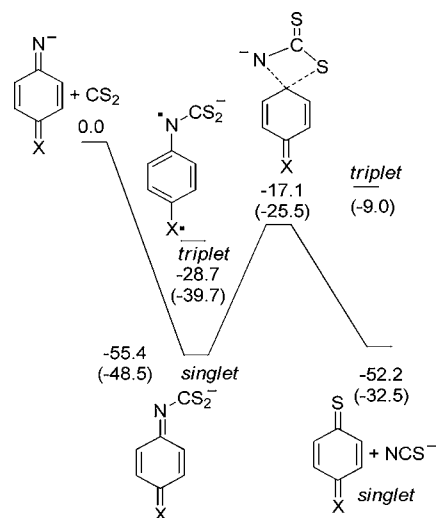
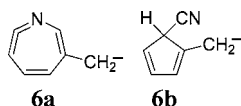


**Figure 2.** Potential energy surface (B3LYP/6-31+G\* energies, relative to the closed-shell singlet states, in kcal/mol) depicting the reaction of **1** and **2** with CS<sub>2</sub>, resulting in the formation of NCS<sup>–</sup>.

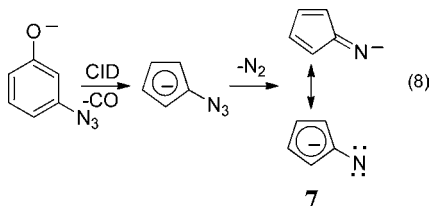
ment barrier for **1** are indicated without parentheses. As with the NO reaction, the energy needed to overcome the barrier is provided by initial bond formation. The corresponding energies of the points on the potential energy surface for sulfur–nitrogen exchange for the singlet state of **2** are shown in parentheses in Figure 2. If **2** has a triplet ground state, then the formation of NCS<sup>–</sup> requires either that the thiobenzoquinone product is formed in a triplet state, or that an intersystem crossing occurs during the course of the reaction. As shown in Figure 2, formation of the triplet state of the thiobenzoquinone is computed to be slightly exothermic, and therefore is a possible reaction pathway, depending on the energy of the transition state. Alternatively, intersystem crossing can occur in the CS<sub>2</sub> adduct, which has a robust singlet ground state, or during its formation, with the subsequent reaction occurring on the singlet surface. A third possible mechanism involves rapid intersystem crossing in **2** before reaction with CS<sub>2</sub>, which could occur if the energies of the singlet and triplet are very close, regardless of the ground state. If that is the case, then the products observed in the reactions with NO and CS<sub>2</sub> could be state specific, but formed in accordance with the Curtin–Hammett principle.<sup>71</sup>

The formation of NCS<sup>–</sup> in the reactions of **1** and **2** with CS<sub>2</sub> is consistent with the presence of negative charge on the nitrogen atoms. In contrast, the reaction of ion **3** with CS<sub>2</sub> results only in formation of adduct. Similarly, addition is the only product observed for the reaction of **3** with NO. Thus, the reactivity of **3** with CS<sub>2</sub> is consistent with that expected for a closed-shell carbanion, but not an open or closed-shell nitrene anion. We propose that the structure of

3 results from rearrangement upon loss of nitrogen, as would be expected in the decomposition of an aromatic azide. Possible structures for the rearrangement product include a keteneimine-like product, **6a**, a ring-contracted cyclopentadiene structure, **6b**, or ions that have rearranged further.



CID of deprotonated *m*-azidotoluene produces **3** as a major product but also produces small amounts of  $[3\text{-HCN}]^-$ . The loss of HCN is more consistent with the presence of **6b** than the corresponding keteneimine, suggesting that **3** rearranges by ring-contraction, although other options are still possible. Deprotonated *m*-azidophenol does not lose nitrogen to any appreciable extent but instead undergoes a net loss of  $\text{CON}_2$ . We observe loss of *m/z* 28 as a minor fragment upon CID of deprotonated *m*-azidophenol, but again the major product corresponds to loss of  $\text{CON}_2$ . Given that phenoxide ions are known to dissociate by loss of CO to form cyclopentadienide upon CID,<sup>72</sup> a possible explanation for the observed results is that *m*-azidophenoxide dissociates by initial loss of CO to form an azidocyclopentadienide, which rapidly decomposes to the cyclopentadienyl nitrene anion, **7** (eq 8).



A computational study has been carried out to obtain additional insight into the effects of substituents on the electron structure of aromatic nitrenes. Natural resonance theory (NRT) analysis<sup>S2–S4</sup> of the closed-shell singlet wave functions (Table 2) supports the qualitative assessment of the effects of  $\pi$ -donating groups expected given the resonance model shown in Figure 1. Stabilization of the singlet states can be attributed to an increase in the extent to which the quinoidal resonance structures (Figure 1b) contribute to the wave function. Indeed, NRT calculations show that those systems for which the singlet state is more stable generally have more resonance contributions from structures that resemble a deprotonated imine, as opposed to a monovalent nitrogen (a nitrene, Figure 1a). Thus, nitrenes with very high singlet energies, such as phenyl nitrene, have less contribution from the imine-like structures, whereas those with more stable singlets are more imine-like. However, even in structures with relatively high energy singlets, the imine-like resonance structure is the major structure. For example, the singlet states of the hydroxy-substituted nitrene or the benzoate are predominantly deprotonated imine-like structures, with less than 25% of the resonance structures corresponding to the nitrene, despite the singlets being more than 20 kcal/mol higher in energy than the triplets.

Table 2 also shows results for some nonphenyl nitrene systems. Cyclopentadienyl nitrene anion, **7**, is an aromatic nitrene that is also predicted to have a closed-shell singlet ground state. As shown in Table 2, the contribution from the deprotonated fulvenimine structure (eq 8) is similar to the quinoidal contributions in **1** and **2**, consistent with **7** having a

small singlet–triplet splitting. Not surprisingly, deprotonated benzaldehyde imine is calculated to have the largest singlet–triplet splitting, and correspondingly the largest amount of deprotonated imine character, although even for that ion almost 3% of the resonance structures correspond to a nitrene, indicating that it still has some nitrene character.

## CONCLUSION

The results obtained in this work suggest that nitrenes generated from *p*-azidophenoxides and benzyl anions should have dramatically different electronic structures from those obtained from neutral substituted phenyl azides, due to differences between neutral and anionic  $\pi$  donating substituents. Whereas *p*- $\text{CH}_2^-$  substituted phenyl nitrene, **1**, can be viewed as a deprotonated quinomethanimine as shown in eq 1, an NRT analysis indicates that the electronic structures of closed-shell singlet nitrenes should be viewed as combinations of the deprotonated imines and nitrene structures, with the difference being the extent to which each contributes to the wave function. While the singlet state of **2** also has significant deprotonated imine character, it is less than that in **1** due to having a weaker  $\pi$ -donor, such that the singlet state is less stabilized, and the phenyl nitrene with a *para*- $\text{O}^-$  substituent is still a ground state triplet in the gas phase.

As expected, increased contribution of a deprotonated imine resonance structure preferentially stabilizes the closed-shell singlet as compared to other states. However, the results in Table 2 also show that the relative state energies are very sensitive to even small differences in electronic structure, especially for systems such as those described here where the singlet and triplet states are similar in energy. As such, the energetics, including the nature of the electronic ground state, will likely be extremely sensitive to the local environment. Therefore, factors such as solvation, further substitution, or annulations could have a large effect on relative state energies despite small changes in electronic structure, and provide a strategy for tuning the electronic properties of these types of intermediates.

## ASSOCIATED CONTENT

### Supporting Information

Mass spectra for formation and reactions of **1**, **2**, and **3**, a comparison of singlet–triplet splittings calculated using BLYP and B3LYP methods, potential energy surfaces for reactions with NO, additional NRT results, details of the spin-flip calculations of **2**, and optimized geometries and energies for all computed structures. This material is available free of charge via the Internet at <http://pubs.acs.org>.

## AUTHOR INFORMATION

### Corresponding Author

pgw@purdue.edu

### Notes

The authors declare no competing financial interest.

## ACKNOWLEDGMENTS

This work was supported by the National Science Foundation (CHE11-11777). Calculations were carried out using the resources of the Center for Computational Studies of Open-Shell and Electronically Excited Species (iopenshell.usc.edu), supported by the National Science Foundation through the CRIF:CRF program. We also thank Dr. Ekram Hossain for assistance with some of the electronic structure calculations,

and Professors Alex Wei and Lawrence Scott for helpful suggestions.

## REFERENCES

- (1) Borden, W. T.; Gritsan, N. P.; Hadad, C. M.; Karney, W. L.; Kemnitz, C. R.; Platz, M. S. *Acc. Chem. Res.* **2000**, *33*, 765–771.
- (2) Gritsan, N. P.; Platz, M. S. *Adv. Phys. Org. Chem.* **2001**, *36*, 255–304.
- (3) Gritsan, N. P.; Platz, M. S. *Chem. Rev.* **2006**, *106*, 3844–3867.
- (4) Platz, M. S. *Acc. Chem. Res.* **1995**, *28*, 487–492.
- (5) Schuster, G. B.; Platz, M. S. *Adv. Photochem.* **1992**, *17*, 69–143.
- (6) Burdzinski, G. T.; Middleton, C. T.; Gustafson, T. L.; Platz, M. S. *J. Am. Chem. Soc.* **2006**, *128*, 14804–14805.
- (7) Grote, D.; Sander, W. J. *Org. Chem.* **2009**, *74*, 7370–7382.
- (8) Tsao, M.-L.; Platz, M. S. *J. Am. Chem. Soc.* **2003**, *125*, 12014–12025.
- (9) Gritsan, N. P.; Zhu, Z.; Hadad, C. M.; Platz, M. S. *J. Am. Chem. Soc.* **1999**, *121*, 1202–1207.
- (10) Johnson, W. T. G.; Sullivan, M. B.; Cramer, C. J. *Int. J. Quantum Chem.* **2001**, *85*, 492–508.
- (11) Karney, W. L.; Borden, W. T. *J. Am. Chem. Soc.* **1997**, *119*, 1378–1387.
- (12) Sankaranarayanan, J.; Rajam, S.; Hadad, C. M.; Gudmundsdottir, A. D. *J. Phys. Org. Chem.* **2010**, *23*, 370–375.
- (13) Winkler, M. J. *Phys. Chem. A* **2008**, *112*, 8649–8653.
- (14) Kim, S.-J.; Hamilton, T. P.; Schaefer, H. F., III. *J. Am. Chem. Soc.* **1992**, *114*, 5349–5355.
- (15) Hrovat, D. A.; Waali, E. E.; Borden, W. T. *J. Am. Chem. Soc.* **1992**, *114*, 8698–8699.
- (16) Smith, B. A.; Cramer, C. J. *J. Am. Chem. Soc.* **1996**, *118*, 5490–5491.
- (17) Castell, O.; García, V. M.; Bo, C.; Caballol, R. *J. Comput. Chem.* **1996**, *17*, 42–48.
- (18) Kemnitz, C. R.; Karney, W. L.; Borden, W. T. *J. Am. Chem. Soc.* **1998**, *120*, 3499–3503.
- (19) Horner, L.; Christmann, A. *Angew. Chem., Int. Ed. Engl.* **1963**, *2*, 599–608.
- (20) Belloli, R. *J. Chem. Educ.* **1971**, *48*, 422–426.
- (21) Meijer, E. W.; Nijhuis, S.; van Vroonhoven, F. C. B. M. *J. Am. Chem. Soc.* **1988**, *110*, 7209–7210.
- (22) Gronert, S.; Keeffe, J. R.; More O'Ferrall, R. A. *J. Org. Chem.* **2009**, *74*, 5250–5259.
- (23) Geise, C. M.; Hadad, C. M. *J. Org. Chem.* **2000**, *65*, 8348–8356.
- (24) Travers, M. J.; Cowles, D. C.; Clifford, E. P.; Ellison, G. B. *J. Am. Chem. Soc.* **1992**, *114*, 8699–8701.
- (25) Wenthold, P. G. *J. Org. Chem.* **2012**, *77*, 208–214.
- (26) Wijeratne, N. R.; Da Fonte, M.; Ronemus, A.; Wyss, P. J.; Tahmassebi, D.; Wenthold, P. G. *J. Phys. Chem. A* **2009**, *113*, 9467–9473.
- (27) Salem, L.; Rowland, C. *Angew. Chem., Int. Ed. Engl.* **1972**, *11*, 92–111.
- (28) Cullin, D. W.; Soundararajan, N.; Platz, M. S.; Miller, T. A. *J. Phys. Chem.* **1990**, *94*, 8890–8896.
- (29) Cullin, D. W.; Yu, L.; Williamson, J. M.; Platz, M. S.; Miller, T. A. *J. Phys. Chem.* **1990**, *94*, 3387–3391.
- (30) Wentrup, C. *Tetrahedron* **1974**, *30*, 1301–1311.
- (31) Wentrup, C.; Crow, W. D. *Tetrahedron* **1970**, *26*, 3965–3981.
- (32) Pritchina, E. A.; Gritsan, N. P.; Maltsev, A.; Bally, T.; Autrey, T.; Liu, Y.; Wang, Y.; Toscano, J. P. *Phys. Chem. Chem. Phys.* **2003**, *5*, 1010–1018.
- (33) Gritsan, N. P.; Pritchina, E. A. *Mendeleev Commun.* **2001**, *11*, 94–95.
- (34) Brown, K. C.; Corbett, J. F. *J. Chem. Soc., Perkin Trans. 2* **1979**, 308–11.
- (35) Fischer, V.; Mason, R. P. *J. Biol. Chem.* **1984**, *259*, 10284–10288.
- (36) Fischer, V.; West, P. R.; Nelson, S. D.; Harvison, P. J.; Mason, R. P. *J. Biol. Chem.* **1985**, *260*, 11446–50.
- (37) Novak, M.; Martin, K. A. *J. Org. Chem.* **1991**, *56*, 1585–90.
- (38) Soulier, L.; Arpin, N.; Kaouadji, M. *Phytochemistry* **1994**, *35*, 597–9.
- (39) Tripathi, G. N. R. *J. Chem. Phys.* **2003**, *118*, 1378–1391.
- (40) Kwon, S. J.; Yang, H.; Jo, K.; Kwak, J. *Analyst (Cambridge, U. K.)* **2008**, *133*, 1599–1604.
- (41) Liu, X.; Tao, Z.; Li, G. *Shandong Jiancai Xueyuan Xuebao* **1997**, *11*, 207–213.
- (42) Modestov, A. D.; Gun, J.; Savotina, I.; Lev, O. *J. Electroanal. Chem.* **2004**, *565*, 7–19.
- (43) Song, Y. *Spectrochim. Acta, Part A* **2007**, *67A*, 611–618.
- (44) Song, Y. Z.; Xie, J. M.; Song, Y.; Ye, Y. *Russ. J. Phys. Chem. A* **2007**, *81*, 1669–1676.
- (45) Wang, Z.; Li, X.; Wu, Y.; Tang, Y.; Ma, S. *J. Electroanal. Chem.* **1999**, *464*, 181–186.
- (46) Mariam, Y. H.; Chantranupong, L. *J. Comput.-Aided Mol. Des.* **1997**, *11*, 345–356.
- (47) Pallagi, I.; Toro, A.; Horvath, G. *J. Org. Chem.* **1999**, *64*, 6530–6540.
- (48) Marinelli, P. J.; Paulino, J. A.; Sunderlin, L. S.; Wenthold, P. G.; Poutsma, J. C.; Squires, R. R. *Mass Spectrom. Ion Processes* **1994**, *130*, 89–105.
- (49) Su, T.; Chesnavich, W. J. *J. Chem. Phys.* **1982**, *76*, 5183–5185.
- (50) Chapyshev, S. V.; Tomioka, H. *Bull. Chem. Soc. Jpn.* **2003**, *76*, 2075–2089.
- (51) Ryu, B.-Y.; Emrick, T. *Macromolecules* **2011**, *44*, 5693–5700.
- (52) Glendening, E. D.; Badenhop, J. K.; Weinhold, F. *J. Comput. Chem.* **1998**, *19*, 628–646.
- (53) Glendening, E. D.; Weinhold, F. *J. Comput. Chem.* **1998**, *19*, 593–609.
- (54) Glendening, E. D.; Weinhold, F. *J. Comput. Chem.* **1998**, *19*, 610–627.
- (55) Frisch, M. J.; Trucks, G. W.; Schlegel, H. B.; Scuseria, G. E.; Robb, M. A.; Cheeseman, J. R.; Montgomery, J. A., Jr.; Vreven, T.; Kudin, K. N.; Burant, J. C.; Millam, J. M.; Iyengar, S. S.; Tomasi, J.; Barone, V.; Mennucci, B.; Cossi, M.; Scalmani, G.; Rega, N.; Petersson, G. A.; Nakatsuji, H.; Hada, M.; Ehara, M.; Toyota, K.; Fukuda, R.; Hasegawa, J.; Ishida, M.; Nakajima, T.; Honda, Y.; Kitao, O.; Nakai, H.; Klene, M.; Li, X.; Knox, J. E.; Hratchian, H. P.; Cross, J. B.; Bakken, V.; Adamo, C.; Jaramillo, J.; Gomperts, R.; Stratmann, R. E.; Yazyev, O.; Austin, A. J.; Cammi, R.; Pomelli, C.; Ochterski, J. W.; Ayala, P. Y.; Morokuma, K.; Voth, G. A.; Salvador, P.; Dannenberg, J. J.; Zakrzewski, V. G.; Dapprich, S.; Daniels, A. D.; Strain, M. C.; Farkas, O.; Malick, D. K.; Rabuck, A. D.; Raghavachari, K.; Foresman, J. B.; Ortiz, J. V.; Cui, Q.; Baboul, A. G.; Clifford, S.; Cioslowski, J.; Stefanov, B. B.; Liu, G.; Liashenko, A.; Piskorz, P.; Komaromi, I.; Martin, R. L.; Fox, D. J.; Keith, T.; Al-Laham, M. A.; Peng, C. Y.; Nanayakkara, A.; Challacombe, M.; Gill, P. M. W.; Johnson, B.; Chen, W.; Wong, M. W.; Gonzalez, C.; Pople, J. A. *Gaussian 03*; Gaussian, Inc.: Wallingford, CT, 2004.
- (56) Shao, Y.; Molnar, L. F.; Jung, Y.; Kussmann, J.; Ochsenfeld, C.; Brown, S. T.; Gilbert, A. T. B.; Slipchenko, L. V.; Levchenko, S. V.; O'Neill, D. P.; DiStasio, R. A., Jr.; Lochan, R. C.; Wang, T.; Beran, G. J. O.; Besley, N. A.; Herbert, J. M.; Lin, C. Y.; Voorhis, T. V.; Chien, S. H.; Sodt, A.; Steele, R. P.; Rassolov, V. A.; Maslen, P. E.; Korambath, P. P.; Adamson, R. D.; Austin, B.; Baker, J.; Byrd, E. F. C.; Dachselt, H.; Doerksen, R. J.; Dreuw, A.; Dunietz, B. D.; Dutoi, A. D.; Furlani, T. R.; Gwaltney, S. R.; Heyden, A.; Hirata, S.; Hsu, C.-P.; Kedziora, G.; Khalliulin, R. Z.; Klunzinger, P.; Lee, A. M.; Lee, M. S.; Liang, W.; Lotan, I.; Nair, N.; Peters, B.; Proynov, E. I.; Pieniazek, P. A.; Rhee, Y. M.; Ritchie, J.; Rosta, E.; Sherrill, C. D.; Simmonett, A. C.; Subotnik, J. E.; Woodcock, H. L., III; Zhang, W.; Bell, A. T.; Chakraborty, A. K.; Chipman, D. M.; Keil, F. J.; Warshel, A.; Hehre, W. J.; Schaefer, H. F., III; Kong, J.; Krylov, A. I.; Gill, P. M. W.; Head-Gordon, M. *Phys. Chem. Chem. Phys.* **2006**, *8*, 3172–3191.
- (57) Wenthold, P. G.; Hu, J.; Squires, R. R. *J. Mass Spectrom.* **1998**, *33*, 796–802.
- (58) Staneke, P. O.; Grootuis, G.; Ingemann, S.; Nibbering, N. M. M. *J. Phys. Org. Chem.* **1996**, *9*, 471–486.

(59) Chacko, S. A.; Wenthold, P. G. *Mass Spectrom. Rev.* **2006**, *25*, 112–126.

(60) Because NO also has a dipole moment (0.15872 debye), the adduct could also be an electrostatically bound complex. Collision-induced dissociation of NO adducts typically occurs only by facile NO loss, consistent with noncovalent interactions. Moreover, although NO addition is also commonly observed with open-shell anions, CID again occurs typically by loss of NO only, indicating that the adduct is likely not an intermediate of a more extensive reaction.

(61) Travers, M. J.; Cowles, D. C.; Ellison, G. B. *Chem. Phys. Lett.* **1989**, *164*, 449–455.

(62) Wenthold, P. G.; Hu, J.; Squires, R. R. *J. Am. Chem. Soc.* **1994**, *116*, 6961–2.

(63) Wenthold, P. G.; Squires, R. R. *J. Am. Chem. Soc.* **1994**, *116*, 11890–7.

(64) Kato, S.; Lee, H. S.; Gareyev, R.; Wenthold, P. G.; Lineberger, W. C.; DePuy, C. H.; Bierbaum, V. M. *J. Am. Chem. Soc.* **1997**, *119*, 7863–7864.

(65) Hammad, L. A.; Wenthold, P. G. *J. Am. Chem. Soc.* **2003**, *125*, 10796–10797.

(66) Chacko, S. A.; Wenthold, P. G. *J. Org. Chem.* **2007**, *72*, 494–501.

(67) Wijeratne, N. R.; Wenthold, P. G. *J. Org. Chem.* **2007**, *72*, 9518–9522.

(68) Wijeratne, N. R.; Wenthold, P. G. *J. Org. Chem.* **2007**, *72*, 9518–9522.

(69) Alternatively, ion **2** could have a singlet ground state with a thermally populatable triplet state, which would indicate the triplet state is within ca. 1–2 kcal/mol.

(70) Barlow, S. E.; Bierbaum, V. M. *J. Chem. Phys.* **1990**, *92*, 3442–3447.

(71) Curtin, D. Y. *Rec. Chem. Prog.* **1954**, *15*, 111–128.

(72) Wenthold, P. G.; Wierschke, S. G.; Nash, J. J.; Squires, R. R. *J. Am. Chem. Soc.* **1994**, *116*, 7378–7392.